JSST
Journal of Space Science & Technology

Vol. 3, No. 3 & 4, Fall 2010 and Winter 2011
pp. 59-67

Application of the Simple Pendulum Model to Incorporate Propellant Slosh Dynamics in 6-DoF Launcher Flight

E. Amani[1], M. Ebrahimi[2*] and J. Roshanian[3]

1, 2. Aerospace Research Institute

3. Department of Aerospace Engineering, K. N. Toosi University of Technology

* Shahrake Ghods, Ave. Mahestan, Tehran, IRAN

mebrahimi@ari.ac.ir

The coupled rigid-body/slosh/elasticity dynamics equations are developed for 6-DoF flight of launchers. The equations of motion are derived by means of Lagrange's equations in terms of quasi-coordinates and alternatively in the inertial frame. The simple pendulum model for planar motion is extended to model slosh dynamics in 6-DoF flight and the elastic motion is represented in terms of modal displacement coordinates relative to the elastic mean axes system. It is shown that this model is consistent with the simpler model for planar motion which has been developed in previous studies. The proposed dynamics model is incorporated in conjunction with the models for the other subsystems in a MATLAB/Simulink program to simulate 6-DoF flight of launchers.

Keywords: slosh, launcher, liquid propellant tank, equations of motion, 6 DOF

Nomenclature

Latin Symbols

C	:	Damping constant
D	:	Dissipation function
d	:	Tank diameter
$\mathbf{e}$	:	Deformation vector
F	:	Thrust
F_2	:	Control engine force
$\mathbf{g}$	:	Gravitational acceleration vector
H	:	Hinge point distance from the liquid center of mass
h	:	Liquid height from bottom of tank
I	:	Moment of inertia
$\mathbf{l}$	:	Slosh vector
$\mathbf{l}_0$	:	Slosh vector in the equilibrium state
L	:	Pendulum length
M	:	Generalized mass of the whole system
m	:	Mass (without index: total mass of system)
N	:	Number of modes
$\mathbf{Q}$	:	Generalized force
$\mathbf{R}$	:	Center of mass position vector with respect to the origin of the inertial frame
$\mathbf{r} = (x, y, z)$	:	Position vector with respect to the origin of the body frame
$\mathbf{r}_0$	:	Initial position vector in the body frame (without deformation)
T	:	Kinetic energy
t	:	Time
U	:	Potential energy
$\mathbf{V} = (u, v, w)$	:	Center of mass velocity with respect to the inertial frame
W	:	Virtual work

Greek symbols

β	:	Control engine angle
γ	:	Slosh damping ratio
η	:	Deformation generalized coordinate
$\mathbf{\Theta} = (\phi^{Eu}, \theta^{Eu}, \psi^{Eu})$	:	Euler angles
λ	:	Deformation damping ratio
ρ	:	Density
$\mathbf{\Phi}$	:	Deformation mode shape function
ψ	:	The angle of pendulum with the negative x direction
$\boldsymbol{\omega} = (p, q, r)$	:	Angular velocity of the body frame with respect to the inertial frame

1. PhD Student
2. Assistant Professor (Corresponding Author)
3. Associate Professor

ω	:	Natural frequency
		Subscripts
0	:	Rigid mass, state of equilibrium with no deformation
B	:	Body frame
E	:	Engine
e	:	Elastic
g	:	Gravitational
i	:	i^{th} deformation mode
j	:	j^{th} tank
k	:	k^{th} slosh mode
liq	:	Liquid
r	:	r^{th} coordinate direction
s	:	Slosh
st	:	Launcher structure
		Other
Bold letter	:	Vectorial quantity
$[\![\ \ ]\!]$	:	Matrix representation of tensor quantity

Introduction

Oscillation of liquid free surface in a tank is called slosh. This phenomenon is observed in launchers, liquid fuel rockets, liquid transport equipments, etc. Slosh induces oscillatory forces and moments on the container. Therefore, accurate slosh dynamics modeling is a crucial task in vehicles which have a large fraction of their weights as liquid. For example in launchers, if the dominant slosh frequencies are close to any of the control system frequencies, instability in the flight characteristics can result. Such problems were reported by NASA in the Jupiter IRBM flight (1957 April 26), the Falcon I flight (2007 March 21), etc.

The governing equations and principals of surface waves, focusing on propellant slosh in space vehicle tanks, have been reviewed in Refs. [1-3] where analytical solutions to slosh problem in tanks with various geometries have also been collected. Equivalent mechanical systems were used by Graham [4] for the first time and after that by many other researchers for modeling slosh dynamics. The parameters of these systems for tanks with different geometries were presented by Abramson et al. [1, 5], Bauer [6], Dodge and Kana [7], Lawrence et al. [8], Lomen [9] and others. The validity of equivalent mechanical models was confirmed by many experimental studies, e.g. [7, 10]. Recently, new experimental methods for determining equivalent mechanical system parameters were proposed by Schlee et al. [11] and Odhekar et al. [12].

In the next step of modeling, liquids can be replaced with equivalent mechanical systems to incorporate propellant slosh dynamics into the system dynamics and stability analysis. Equations governing motion of space vehicles can be categorized in several subsystems. They include dynamics, control, and guidance subsystems. Dynamics subsystem is itself composed of rigid body, elasticity, and slosh dynamics equations.

From classical studies concerning the derivation of equations of motion for an elastic vehicle the works by Meirovitch and coworkers [13-15] can be pointed out. Recently, Bilimoria and Schmidt [17] developed a framework for integrated modeling of the motion of flight vehicles. They derived the coupled rigid-body/elasticity equations including internal fluid flow, rotating machinery, wind, and a spherical rotating Earth model.

In all of the above studies, the slosh dynamics has not been considered. In contrast to coupled rigid-body/aeroelasticity studies, fewer studies have been devoted to integrated modeling of the three dynamic subsystems, namely the slosh, rigid-body, and aeroelasticity. From the earliest studies in this context, a model using many simplifications, including planar motion and neglecting centrifugal and coriolis forces, was reported in ref. [1]. Recently, Shekhawat et al. [18] derived the integrated rigid-body/slosh dynamics equations for a rigid vehicle in planar motion and investigated the effect of slosh parameters on the stability of the vehicle. There is no published study considering elasticity and slosh dynamics for a 6-DoF flight, as the best of our knowledge.

In the following sections, first, an equivalent mechanical system based on series of simple pendulum is introduced to model propellant slosh. Then, a model is proposed to incorporate propellant slosh dynamics in the equations of motion for 6-DoF launcher flight by extending the simple pendulum model in planar motion. The elasticity of launcher is also considered in the derivation. As a validation, the consistency of the proposed model is checked with the simpler model which has been reported in other studies. Then, the proposed model is employed to simulate the flight of a launcher. Some of the results of an extensive study on the model performance are reported here.

Slosh Modeling

Equivalent mechanical systems are employed to incorporate slosh effect on the launcher dynamics equations. An equivalent mechanical system exerts the same net force and moment on the tank structure as the net force and moment exerted by the sloshing liquid. Furthermore, total mass, moments of inertia, center of mass location, and the damping effect are also the same. For more information about the properties of equivalent mechanical models consult Refs. [19, 2]. Before determining the parameters of an equivalent mechanical system, the slosh force and moment have to be determined. This is provided by solution of the equations, which govern motion of the sloshing liquid, via analytical or numerical methods or alternatively by experiments.

Different mechanical models have been presented for slosh modeling in literatures. Here, we choose the simple pendulum model for lateral sloshing, the liquid in the jth tank is replaced by N_s simple pendulums and also a rigid mass, m_{j0}, with the moment of inertia, $[\![I_{j0}]\!]$, attached to the launcher structure (see Fig. 1). Each pendulum represents one slosh mode and has four parameters including the point mass, m_{jk}, pendulum length, L_{jk}, hinge point distance from the liquid center of mass, H_{jk}, and damping constant, C_{jk} [2, 19 and 20].

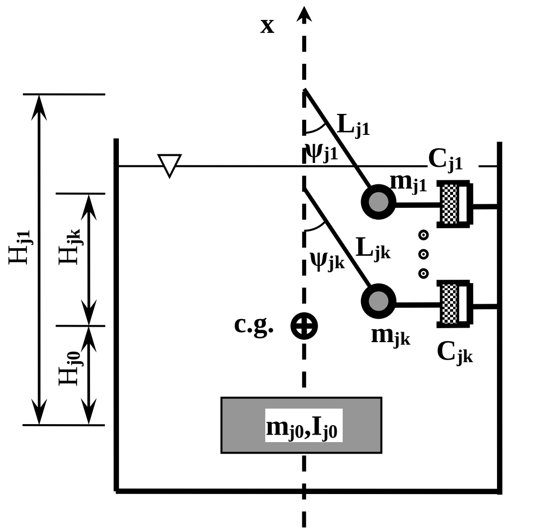

Fig.1 Equivalent mechanical system (simple pendulum) for liquid in the jth tank.

In the case of cylindrical tanks which are selected here as launcher propellant tanks, there is analytical solution for the linear slosh governing equations. It can be shown that the parameters of the equivalent pendulum system are [19, 21]

$$m_{jk} = m_{1iq,j}\left[\frac{\tanh(2\xi_k h_j/d_j}{(\xi_k^2-1)\xi_k h_j/d_j}\right],\ m_{liq,j} = \frac{\pi}{4}\rho_j h_j d_j^2$$

$$L_{jk} = \frac{d_j}{2\xi_k \tanh(2\xi_k h_j/d_j)}, H_{jk} = L_{jk} + \frac{h_j}{2} - \frac{d_j \tanh(\xi_k h_j/d_j)}{\xi_k}$$

$$m_{j0} = m_{liq,j} - \sum_k m_{jk}, H_{j0} = -\frac{\sum_k m_{jk}(H_{jk}-L_{jk})}{m_{j0}}$$

$$I_{y,j0} = m_{liq,j}\left(\frac{h_j^2}{12} + \frac{d_j^2}{16}\right) - 2m_{liq,j}d_j^2 \sum_k \frac{[1-d_j/(\xi_k h_j)]\tanh(\xi_k h_j/d_j)}{(\xi_k^2-1)\xi_k^2} - m_{j0}h_{j0}^2 - \sum_k m_{jk}\left(H_{jk}-L_{jk}\right)^2 \tag{1}$$

where, d_j is the diameter of the j^{th} tank and ρ_j, $m_{liq,j}$, and h_j are the liquid density, mass, and height in the j^{th} tank, respectively. ξ_k is the k^{th} root of the Bessel function derivative of the first kind and of order one.

Above model is for lateral liquid sloshing due to tank excitation (translational and rotational) in directions parallel to liquid free surface in its equilibrium state. In tanks with axially symmetric shapes, the rolling motion about the axis doesn't create liquid sloshing but the relative rolling motion of liquid with respect to tank walls dissipates energy. This phenomenon, which is important in spin-stabilized space vehicles, is neglected here. In reference [22] a model has been presented to include this effect in dynamics equations. Translational excitation normal to liquid free surface also causes another kind of sloshing which is called vertical or parametric sloshing. This kind of sloshing is usually negligible [19, 2] and is omitted here.

Launcher Dynamics Equations

Dynamics equations can be derived by determining kinetic energy, T, potential energy, U, and dissipation function, D, of the system and utilizing Lagrange's equation for each generalized coordinate, q_i. Lagrange's equation is classically written in the inertial frame as

$$\frac{d}{dt}\left[\frac{\partial(T-U)}{\partial\dot{q}_i}\right] - \frac{\partial(T-U)}{\partial q_i} + \frac{\partial D}{\partial\dot{q}_i} = Q_{q_i} \tag{2}$$

Then, the resultant equations are transformed into the body frame. Alternatively, Lagrange's equation in terms of quasi-coordinates, also called Boltzmann-Hamel equation, can be utilized that directly results in equations which are in the body frame. Both methods were employed here and the same set of equations was obtained in both cases. For details of the derivation, please refer to Ref. [22].

Assuming linear slosh regime, the lateral sloshing in the pitch and yaw channels can be included independently. For this purpose, it is assumed here that two sets of simple pendulums are used. For cylindrical tanks, the parameters of these two sets are the same which are calculated by Eq.(1). The pendulums of the first set oscillate in $x-z$ plane with the slosh angle $(\psi_z)_{jk}$ and affect only the motion in the pitch channel while the pendulums of the second set oscillate in $x-y$ plane with the angle $(\psi_y)_{jk}$ and affect only the yaw motion. One representative pendulum of each set is shown in Fig. 2.

The following definitions are used;

$$\mathbf{r} = \mathbf{r}_0 + \mathbf{e} + \mathbf{l} \tag{3}$$

where, $\mathbf{r}$ is the position vector of each point of the system with respect to the origin of the body frame. For a slosh mass, $\mathbf{r}_0$ is the initial position (without deformation) of its hinge point, $\mathbf{e}$ is the deformation vector of this point, and $\mathbf{l}$ is the slosh vector which is the vector from the hinge point to the slosh point mass. For the launcher structure, $\mathbf{r}_0$ is the initial position of each point, $\mathbf{e}$ is the deformation vector, and $\mathbf{l} = 0$.

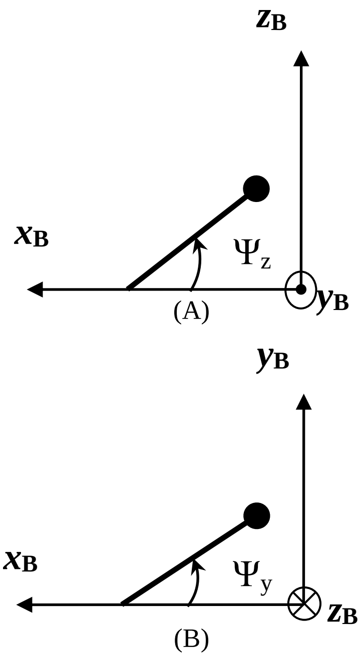

Fig.2 Representative simple pendulum oscillating in a specific channel. (A): in the pitch channel, (B): in the yaw channel.

Here, the launcher center of mass is defined as the center of mass of all masses in their equilibrium states $(\mathbf{e} = \mathbf{0}, \mathbf{l} = \mathbf{l}_0)$, where $\mathbf{l}_0$ indicates equilibrium position of the slosh masses. Therefore,

$$\int_m (\mathbf{r}_0 + \mathbf{l}_0)\, dm = 0 \tag{4}$$

where, the integration region m indicates the integration on the whole system masses. Selecting Cartesian coordinates, the following definitions are used

$$\mathbf{r} = x\,\mathbf{i}_B + y\,\mathbf{j}_B + z\,\mathbf{k}_B \tag{5}$$

$$\mathbf{r}_0 = x_0\,\mathbf{i}_B + y_0\,\mathbf{j}_B + z_0\,\mathbf{k}_B \tag{6}$$

$$\mathbf{V} = u\,\mathbf{i}_B + v\,\mathbf{j}_B + w\,\mathbf{k}_B \tag{7}$$

$$\boldsymbol{\omega} = p\,\mathbf{i}_B + q\,\mathbf{j}_B + r\,\mathbf{k}_B \tag{8}$$

$$\mathbf{l} = l_x\,\mathbf{i}_B + l_y\,\mathbf{j}_B + l_z\,\mathbf{k}_B \tag{9}$$

$$\mathbf{e} = e_x\,\mathbf{i}_B + e_y\,\mathbf{j}_B + e_z\,\mathbf{k}_B \tag{10}$$

$$\mathbf{g} = g_x\,\mathbf{i}_B + g_y\,\mathbf{j}_B + g_z\,\mathbf{k}_B \tag{11}$$

$$[\![I]\!] = \begin{bmatrix} I_x & -I_{xy} & -I_{xz} \\ -I_{yx} & I_y & -I_{yz} \\ -I_{zx} & -I_{zy} & I_z \end{bmatrix} = \int_m \begin{bmatrix} y^2+z^2 & -xy & -xz \\ -xy & x^2+z^2 & -yz \\ -xz & -yz & x^2+y^2 \end{bmatrix} dm \tag{12}$$

where, $\mathbf{V}$ is the center of mass velocity with respect to the inertial frame, $\boldsymbol{\omega}$ is the angular velocity of the body frame with respect to the inertial frame, $\mathbf{g}$ is the gravitational acceleration vector, $[\![I]\!]$ is the moment of inertia tensor. The subscript B indicates the components of a vector in the Cartesien body coordinates.

For elasticity equations, it is usually assumed that

$$\mathbf{e} = \sum_{i=1}^{\infty} \eta_{x,i}(t)\ \phi_{x,i}(\mathbf{r})\ \mathbf{i}_B + \sum_{i=1}^{\infty} \eta_{y,i}(t)\ \phi_{y,i}(\mathbf{r})\ \mathbf{j}_B + \sum_{i=1}^{\infty} \eta_{z,i}(t)\ \phi_{z,i}(\mathbf{r})\ \mathbf{k}_B \tag{13}$$

where, $\phi_{r,i}$ is the i^{th} mode shape function of the r^{th} coordinate direction $(r = x, y, z)$ which is a function of position and $\eta_{r,i}$ is the i^{th} generalized coordinate of deformation in the r^{th} coordinate direction and is a function of time, only. The body axes are selected as the mean axes wherein for an elastic body, the relative linear and angular momentums due to elastic deformation are zero at every instant, namely [16, 17]

$$\int_m \dot{\mathbf{e}}\, dm = 0 \tag{14}$$

$$\int_m \mathbf{r} \times \dot{\mathbf{e}}\, dm = 0 \tag{15}$$

It is also assumed that the following assumptions are held

$$v \le u, w \quad , \quad \dot{v} \le \dot{u}, \dot{w} \quad , \quad r, p \le q \quad , \quad \dot{r}, \dot{p} \le \dot{q} \tag{16}$$

where, $\ll \dot{} \gg$ sign indicates the time derivative in the body frame. The above assumption is true for a non-spinning stabilized launcher which its programmed motion is dominantly in $x - z$ plane. In other words, the equations are simplified assuming this trim state.

The dynamics equations of motion can be derived with the following assumptions as [22]

Velocity (rigid body dynamics)

$$m \begin{Bmatrix} \dot{u} \\ \dot{v} \\ \dot{w} \end{Bmatrix} + m \begin{Bmatrix} qw - rv \\ ru - pw \\ pv - qu \end{Bmatrix} + \sum m_{jk} L_{jk} \begin{Bmatrix} 0 \\ \ddot{\psi}_y \\ \ddot{\psi}_z \end{Bmatrix}_{jk} + \sum m_{jk} L_{jk} \begin{Bmatrix} 0 \\ -(r^2+p^2)\psi_y \\ -q^2\psi_z \end{Bmatrix}_{jk} - m \begin{Bmatrix} g_x \\ g_y \\ g_z \end{Bmatrix} = \mathbf{Q_V} \tag{17}$$

Angular velocity (rigid body dynamics)

$$\begin{Bmatrix} I_x\dot{p} + \dot{I}_x p \\ I_y\dot{q} + \dot{I}_y q \\ I_z\dot{r} + (I_y - I_x)pq + \dot{I}_z r \end{Bmatrix} +$$
$$\sum m_{jk} L_{jk} \begin{Bmatrix} 0 \\ \dot{u}\psi_z - (x_0 - L)\ddot{\psi}_z \\ -\dot{u}\psi_y + (x_0 - L)\ddot{\psi}_y \end{Bmatrix}_{jk} +$$
$$\sum m_{jk} L_{jk} \begin{Bmatrix} 0 \\ wq\psi_z \\ -wq\psi_y \end{Bmatrix}_{jk} +$$
$$g \sum m_{jk} \begin{Bmatrix} 0 \\ L\psi_z \cos\phi^{Eu} \sin\phi^{Eu} \sin\theta^{Eu} \\ -L\psi_y \sin^2\phi^{Eu} \sin\theta^{Eu} \end{Bmatrix}_{jk} +$$
$$\left[\sum m_{jk} L_{jk} \begin{Bmatrix} 0 \\ 0 \\ qe_z\dot{\psi}_y \end{Bmatrix}_{jk} \right] = \mathbf{Q}_{\boldsymbol{\omega}} \tag{18}$$

where, $(\phi^{Eu}, \theta^{Eu}, \psi^{Eu})$ are the Euler angles which describe the orientation of the body frame relative to the vehicle-carrying frame in the standard aircraft (3-2-1) Euler sequence [17] and the sums are over all slosh masses.

For each sloshing mass, m_{jk}, (slosh dynamics)

$$L\ddot{\psi}_z + 2\gamma_{\psi_z}\omega_{\psi_z}L\dot{\psi}_z + \{(\dot{u} - g_x) + (qw - q^2x_0) - [2q\dot{e}_z + \dot{q}e_z]\}\,\psi_z + \{(\dot{w} - g_z) - \dot{q}(x_0 - L) - qu + [\ddot{e}_z - q^2 e_z]\} = 0 \tag{19}$$

$$L\ddot{\psi}_y + 2\gamma_{\psi_y}\omega_{\psi_y}L\dot{\psi}_y + \{(\dot{u} - g_x) + qw - q^2(x_0 + L) + [2q\dot{e}_z + \dot{q}e_z]\}\,\psi_y + \{(\dot{v} - g_y) - ru + \dot{r}(x_0 - L) + pqx_0 + [\ddot{e}_z - 2p\dot{e}_z + rqe_z]\} = 0 \tag{20}$$

where, ω_{jk} is the slosh frequency of the k^{th} slosh mode in the j^{th} tank, γ_{ψ_z} and γ_{ψ_y} are the slosh damping ratios. In Eqs.(19) and (20), for the variables ψ_z, ψ_y, L, x_0, γ_{ψ_z}, γ_{ψ_y}, ω_{ψ_z}, and ω_{ψ_y} the subscript jk is dropped for clarity of the equations.

For accurate determination of elastic deformation, the distribution of slosh forces and moments acting on the launcher body should be considered in the aeroelasticity equations. Therefore, usage of equivalent mechanical systems, where distributed forces and moments are replaced by concentrated ones, is not appropriate in this case. These distributions are not usually available, hence as an approximation, equivalent mechanical models have been used for the derivation of aeroelastic equations in some literatures, e.g. [2, 22]. With this approximation, elasticity equations can be derived as

Elasticity equations

$$(20)\, M_{x,i}\ddot{\eta}_{x,i} + M_{x,i}\lambda_{x,i}\omega_{e,x,i}\dot{\eta}_{x,i} + M_{x,i}\omega_{e,x,i}^2\eta_{x,i} = Q_{\eta_{x,i}}$$

$$M_{y,i}\ddot{\eta}_{y,i} + M_{y,i}\lambda_{y,i}\omega_{e,y,i}\dot{\eta}_{y,i} + M_{y,i}\omega_{e,y,i}^2\eta_{y,i} + \left[\sum m_{jk}\left(L\ddot{\psi}_y\Phi_{y,i}\right)_{jk}\right] = Q_{\eta_{y,i}} \tag{21}$$

$$M_{z,i}\ddot{\eta}_{z,i} + M_{z,i}\lambda_{z,i}\omega_{e,z,i}\dot{\eta}_{z,i} + M_{z,i}\omega_{e,z,i}^2\eta_{z,i} + \left[\sum m_{jk}\left(L\ddot{\psi}_z\Phi_{z,i}\right)_{jk}\right] = Q_{\eta_{z,i}} \tag{22}$$

where, $\omega_{e,r,i}$ is the deformation frequency of the i^{th} mode and of the r^{th} coordinate direction and $M_{r,i}$ is the i^{th} generalized mass of the whole system and of the r^{th} coordinate

$$M_{r,i} = \int_m \phi_{r,i}\,\phi_{r,i}\,dm \tag{23}$$

The second approximation is to consider the whole system as an (equivalent) elastic solid body [23]. By this approximation, the terms in brackets are eliminated in Eq.(20)-(23).

Consistency

In this section, as a validation of our results, we simplify our equations with the assumptions used in the previous works and show that our equations are consistent with the previous models. For example, the dynamics equations of an elastic vehicle in 6-DoF motion without propellant sloshing were derived using different assumptions [17, 16 and 23]. Omitting all the slosh terms in the dynamics equations of section 3, the results of the corresponding references are recovered. Consistency check with another literature [2] is reported in the following.

Planar motion of an elastic launcher

In this section, as a validation of our results, we simplify our model with the assumptions which were used in the study by Dodge [2] and show that our equations are consistent in this simplified case.

Dodge [2] assumed:

1. The planar motion in $x - z$ plane.
2. Centrifugal and coriolis forces are negligible.
3. Small disturbances.
4. The gravity vector is in the negative x direction ($\mathbf{g} = -g\,\mathbf{i}_B$).
5. The vehicle is slender hence every quantity is assumed as a function of the x coordinate.

The thrust force, F, is decomposed to an axial, F_1, and a control force, F_2, which has the angle β with the negative x direction as shown in Fig.3.

$$F = F_1 + F_2 \tag{24}$$

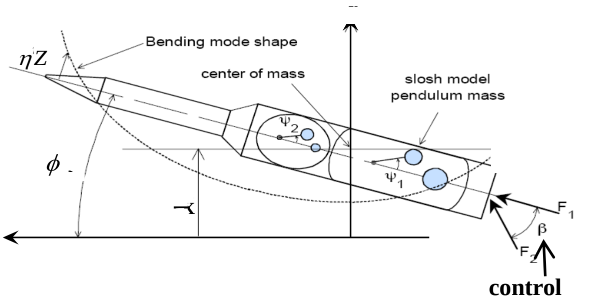

Fig.3 Schematic configuration of different subsystems in a launcher (from Ref. [2] with some modifications).

This relation is held for small oscillations ($\cos\phi \sim \cos\beta \sim 1$). It should be noted that $\dot{\phi} = -q$ in Fig.3. The generalized forces are [2]

$$Q_u = F \tag{25}$$

$$Q_w = F\left\{\phi + \sum_{i=1}^{\infty} \eta_i \left.\frac{d\Phi_{z,i}}{dx}\right|_{x_{0,E}}\right\} + F_2\beta \tag{26}$$

$$Q_\phi = -Q_q = F\left\{x_{0,E} \sum_{i=1}^{\infty} \eta_i \left.\frac{d\Phi_{z,i}}{dx}\right|_{x_{0,E}} + \sum_{i=1}^{\infty} \eta_i\, \Phi_{z,i}(x_{0,E})\right\} + F_2 x_{0,E}\beta \tag{27}$$

$$Q_{\eta_i} = F_2\beta\, \Phi_{z,i}(x_{0,E}) \tag{28}$$

where, $x_{0,E}$ is the location of the control engine nozzle with respect to launcher center of mass. Aerodynamic forces are neglected.

Employing the above simplifications in Eqs.(17)-(24), one can obtains

$$m\begin{Bmatrix}\dot{u}+g\\ \dot{w}\end{Bmatrix} + \sum m_{jk}\begin{Bmatrix}0\\ L\ddot{\psi}\end{Bmatrix}_{jk} = \begin{Bmatrix}Q_u\\ Q_w\end{Bmatrix} \tag{29}$$

$$I_y\ddot{\phi} - (\dot{u}+g)\sum m_{jk}(L\psi)_{jk} + \sum m_{jk}\left[L\ddot{\psi}(x_0 - L)\right]_{jk} = Q_\phi \tag{30}$$

$$L\ddot{\psi} + 2L\gamma_\psi\omega_\psi\dot{\psi} + (\dot{u}+g)\psi = -\left[\dot{w} + \ddot{\phi}(x_0 - L) + \ddot{e}_z\right] \tag{31}$$

$$\ddot{\eta}_i + \lambda_i\omega_i\dot{\eta}_i + \omega_i^2\eta_i = \frac{Q_{\eta_i}}{M_i} - \frac{1}{M_i}\sum m_{jk}\left(L\ddot{\psi}\Phi_{z,i}\right)_{jk} \tag{32}$$

These equations are in accordance with the equations which were derived in Ref. [2]. The only difference is due to the assumptions for the body axes and deformation. In that reference, the body axes has not been selected as the mean axes. And for the elasticity, Eq. (13) has not been assumed. To account for these differences, it is sufficient to add

$$-(\dot{u}+g)\left[\phi + \frac{\partial e_z}{\partial x}\right] \tag{33}$$

to the left-hand side of Eq.(107) and

$$-\frac{1}{M_i}(\dot{u}+g)\sum m_{jk}\left(L\psi\frac{\partial\Phi_{z,i}}{\partial x}\right)_{jk} \tag{34}$$

to the left-hand side of Eq.(108) to recover the equations of Ref. [2], exactly. The model of Ref. [2] (Eqs. (30)- (33)) was also used for the planar launcher flight in authors' previous work [20].

Simulation

The new dynamics model (section 3) in conjunction with the models for other subsystems is used to simulate 6-DoF flight of a launcher via a MATLAB/Simulink program which is named “Simulator”. The modeling approaches for the other subsystems which are used to develop the Simulator program can be found in the other literatures [24-26]. These models are for guidance and navigation, control, aerodynamic and thrust forces, atmospheric properties including the wind effect, elliptical earth model for gravity, etc.

Note that, in this simulation, the second approximation for the elasticity (see section 3) is employed. In addition the slosh/elasticity interaction terms in the dynamics equations are neglected, i.e. in Eqs. (17) - (24), the terms in brackets are neglected. Therefore, the effect of deflection is only considered on aerodynamic forces and moments and on the engine thrust direction.

Simulation is performed for a two-stage launcher with the specification reported below. Only the first stage of flight is considered.

Tank position and launcher sizes: see Fig. 4.

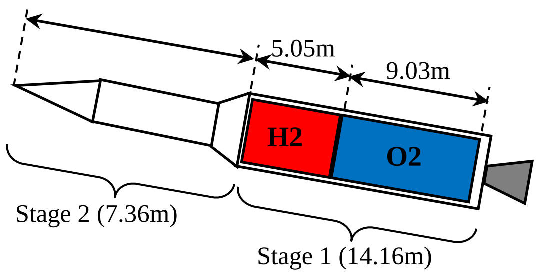

Fig.4 Specification of the Launcher which is used in the simulation.

Tank and launcher masses: The tank diameter is 1.3 m and the initial masses of components are

$$m_{H2} = 5512\ \mathrm{kg}, \quad m_{O2} = 13779\ \mathrm{kg}, \quad m_{st,1^{st}\ stage} = 4576\ \mathrm{kg}$$
$$m_{total,2^{nd}\ stage} = 7135\ \mathrm{kg} \tag{35}$$

It is assumed that the masses of first-stage propellants are consumed at constant rate during the first stage flight (120s).

Moment of inertia tensor and center of masses: These parameters are computed assuming uniform mass distribution for each component (tanks and launcher body are assumed cylindrical).

Engine thrust and aerodynamic forces: This information includes many parameters, including 29 aerodynamic coefficients, thrust forces of main and control engines, etc. This information has been reported in Refs. [24, 26].

Guidance and navigation: The guidance command has been designed to change from zero to -0.014 rad/s at about $t = 10s$ and then gradually reduce with constant slopes in the intervals $12s < t < 83s$ and $83s < t < 118s$ (see also the solid line curve in Fig. 5). For more details of this subsystem, one can refer to Ref. [25].

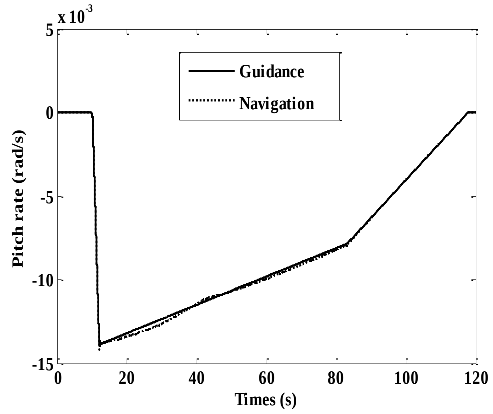

(A)

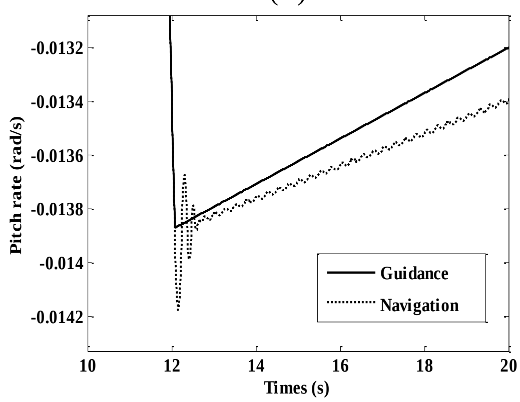

(B)

Fig.5 The pitch rate (q) versus time. Comparison of the guidance command and navigation measurement. (A) figure shows the whole range. (B) figure shows a scaled view.

Now, some results of the simulation in the pitch channel are briefly described. In Fig.5, the pitch rate, q, is depicted during the flight. As observed in this figure, the deviation from the nominal (guidance) curve, which is due to the elasticity and slosh interactions, is negligible. But when the wind effect which exerts oscillatory aerodynamic forces and moments, is included, sever oscillations in the pitch rate are started at $t = 27s$. Two cases are considered in Fig.6. In the first case, slosh is not considered in the modeling and the second case includes slosh effect.

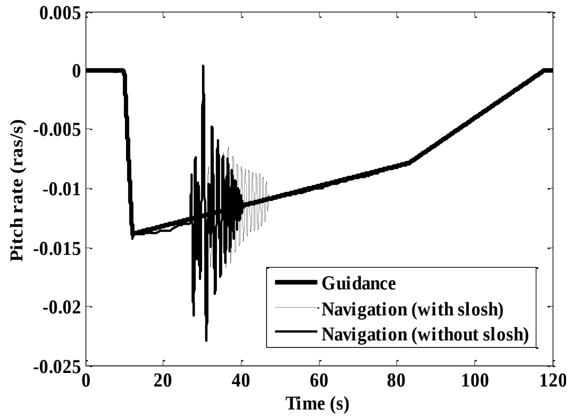

Fig.6 The pitch rate (q) versus time. Aerodynamic wind forces and moments are included. Comparison of the guidance command and navigation measurement for the cases without and with slosh.

When slosh is included, it takes longer time for the system to damp the high amplitude oscillations arise from the wind effect, because the settling time for the sloshing liquid propellant is greater than the settling time for the elastic solid structure. The net slosh moment which is exerted on the launcher in the pitch channel is depicted in Fig.7 for cases with and without the wind effect.

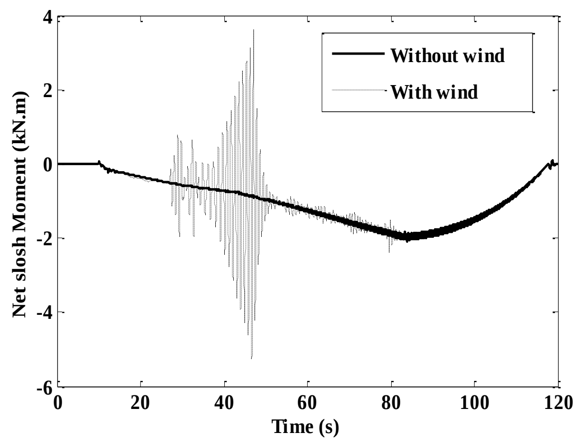

Fig.7 The net slosh moment exerted on the launcher in the pitch channel versus time. Comparison of the cases with and without the wind effect.

The wind velocity which is exerted on the launcher during first stage is reported in Fig.8. The interaction between the wind and slosh causes high amplitude oscillations in the slosh moment. The maximum slosh moment also increases more than 2.5 times.

For the specified launcher, the design of propellant tanks as well as control subsystem were done such that any of the dominant slosh frequencies is not close to the control frequencies, during the first flight stage. Therefore, the oscillations do not amplify and are damped after some time when the (wind) excitation ends.

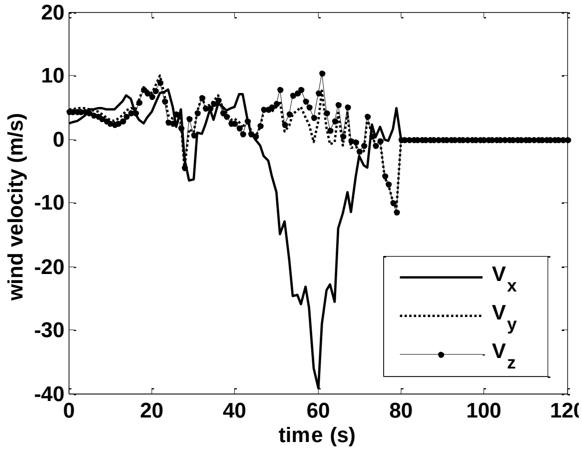

Fig. 8 Wind velocity components in the body coordinates.

Conclusion

The equivalent mechanical system based on series of simple pendulum was introduced to model propellant slosh. Then, the coupled rigid-body/slosh/elasticity dynamics equations were developed by means of Lagrange's equations in terms of quasi-coordinates and simplified with appropriate assumptions. The simple pendulum model for planar motion was extended to model slosh dynamics in 6-DoF flight and the elastic motion was represented in terms of modal displacement coordinates relative to the elastic mean axes system. As a validation, the consistency of the model was checked with a previous simpler model. Finally, to show the application of the proposed model, the flight of a launcher was simulated and the effect of slosh on the launcher dynamics was investigated under a wind excitation.

References

[1] Abramson, H. A., "The Dynamic Behavior of Liquids in Moving Containers", NASA SP-106, 1966

[2] Dodge, F. T., "The New Dynamic Behavior of Liquids in Moving Containers", Southwest Research Institute, 2000.

[3] Ibrahim, R. A., *Liquid Sloshing Dynamics*, Cambridge University Press, 2005.

[4] Graham, E. W., "The Forces Produced by Fuel Oscillations in a Rectangular Tank", Douglas Aircraft Co., SM-13748, 1951

[5] Abramson, H. N., Chu, W. H. and Ransleben, G. E., "Representation of Fuel Sloshing in Cylindrical Tanks by an Equivalent Mechanical Model", *ARS J.*, Vol. 31, No. 12, 1961, pp. 1697-1705

[6] Bauer, H. F., "Theory of the Fluid Oscillation in a Circular Cylindrical Ring Tank Partially Filled with Liquid", NASA TN D-557, 1960

[7] Dodge, F. T. and Kana, D. D., "Moment of Inertia and Damping of Liquids in Baffled Cylindrical Tanks", *J. Spacecraft Rockets*, Vol. 3, No. 1, 1966, pp. 153-155

[8] Lawrence, H. R., Wang, C. J. and Reddy, R. B., "Variational Solution of Fuel Sloshing Modes", *Jet Propulsion*, Vol. 128, No. 11, 1958, pp. 729-736

[9] Lomen, D. O., "Liquid Propellant Sloshing in Mobile Tanks of Arbitrary Shape," NASA CR-222, 1965

[10] Abramson, H. N. and Ransleben, G. E., "Some Comparison of Sloshing Behavior in Cylindrical Tanks with Flat and Conical Bottoms", *ASR J.*, Vol. 31, No. 4, 1961, pp. 542-544

[11] Schlee, K., Gangadharam, S. and Ristow J., "Advanced method to Estimate Fuel Slosh Simulation Parameters", *AIAA paper* 2005-3596, 2005

[12] Odhekar, D. D., Gandhi, P. S. and Joshi, K. B., "Novel Methods for Slosh Parameter Estimation Using Pendulum Analogy", AIAA Paper 2005-5923, 2005

[13] Meirovitch, L. and Wesley, D. A., "On the Dynamic Characteristics of Variable-Mass Slender Body under High Accelerations", *AIAA J.*, Vol. 5, No. 8, 1967, pp. 1439-1447.

[14] Meirovitch, L., "The General Motion of a Variable-Mass Flexible Rocket with Internal Flow", NASA CR-1528, 1970.

[15] Meirovitch, L., "General Motion of a Variable-Mass Flexible Rocket with Internal Flow", *J. Spacecraft and Rockets*, Vol. 7, No. 2, 1970, pp. 186-195.

[16] Waszak, M. R, and Schmidt, D. K, "Flight Dynamics of Aeroelastic Vehicles", *Journal of Aircraft*, Vol. 25, No. 6, 1988, pp 565-571.

[17] Bilimoria, K. D. and Schmidt, D. K., "Integrated Development of the Equations of Motion for Elastic Hypersonic Flight Vehicles", *AIAA J. Guidance, Control and Dynamics*, Vol. 18, No. 1, 1995, pp 73-81.

[18] Shekhawat, A., Nichkawde, C. and Ananthkrishnan, N., "Modeling and Stability Analysis of Coupled Slosh-Vehicle Dynamics in Planar Atmospheric Flight", *44th AIAA Aerospace Sciences Meeting and Exhibit*, 9-12 January 2006, Reno, Neveda.

[19] Amani, E. and Ebrahimi, M., "An Investigation of Liquid Slosh in Fuel Tanks of Launchers", Aerospace Research Institute, Iran, Technical Report: ARI-87-21-LV-SLP-4-1-1, 2009.

[20] Amani, E., Tayefi, M., Ebrahimi, M. and Roshanian, J., "Modeling of Propellant Sloshing to Exert on Flight Simulation of Launch Vehicles", *First Specialist Conference of Flight Simulation*, ARI, Tehran, Iran, 2009.

[21] James, R. R., Eduardo, R. B. and Pei-Ying, C., "Slosh Design Handbook I", NASA CR-406, 1985.

[22] Amani E. and Ebrahimi, M., "Mathematical Modeling of Liquid Propellant Slosh Dynamics for the Application of Launcher Flight Simulation", Aerospace Research Institute, Iran, Technical Report: ARI-89-21-LV-SLP-4-1-1, 2010.

[23] Fathi, M., Abadi, M. T., Tayefi, M. and Razi, M., "Modeling of Aeroelasticity in Launch Vehicles", Aerospace Research Institute, Iran, Technical Report: ARI-87-31-LVAEL-1-1-1, 2009.

[24] Taheri, E., Tayefi, M. and Roshanian, J., "Development of a Space Access Vehicle 6DoF Multipurpose Simulation Software in MATLAB/ Simulink", *Proceedings of the ASME 2010 10th Biennial Conference on Engineering Systems Design and Analysis,* ESDA 2010 July 12-14, 2010, Istanbul, Turkey.

[25] Mohammadi, A., Tayefi, M. and Roshanian J., "Combining the Preset and IGM Methods for the Guidance of Launchers", *IAS2009-MF593, 8th Annual Conference of Iranian Aerospace Society*, Esfahan, 2009.

[26] Taheri, E., Tayefi, M. and Roshanian, J., "Modeling of launcher aerodynamics for 6DoF flight simulation based on MD software", *First Specialist Conference of Flight Simulation*, ARI, Tehran, Iran, 2009.